

# Experimental Verification of Formulas for Variances of Plane Parameters Fitted to Three-Dimensional Imaging Data

Marek Franaszek, Geraldine S. Cheok, and Kamel S. Saidi

**Abstract**—Nonlinear least squares method is applied to fit a plane to 3-D imaging data. Two different error functions used in fitting are tested: orthogonal and directional. Variances of fitted parameters are calculated either from a single data set using derived earlier analytical formulas or by repeating the scans at the same experimental settings. In the latter case, the variance is equal to the square of the standard deviation from the repeated scans. The results show that the orthogonal error function severely underestimates the variances calculated by using the mathematical formulas when compared to the variances calculated from multiple scans. The variances calculated from formulas based on the directional error function are in good agreement with the estimates calculated from multiple scans. Thus, the variances of the fitted plane parameter can be determined correctly from a single scan when proper formulas are used. This is important because multiple scans from the same location are typically not performed in the field.

**Index Terms**—Directional error function, nonlinear least squares (NLS), orthogonal error function, variances of fitted plane parameters, 3-D imaging systems.

## I. INTRODUCTION

THREE-dimensional imaging systems allow rapid measurements of the surface of an object using light reflected from that surface. For the class of instruments in which the detector and emitter lines of sight coincide, the range  $r(\vartheta, \varphi)$  is measured along a ray from the instrument's center to the first intersection of the ray with an object. Parameters  $\vartheta$  and  $\varphi$  are the elevation and the azimuth angles from a reference axis to that point of intersection. The scanning process is very fast, and current systems can collect point clouds containing hundreds of thousands of points within a few seconds [1]. These large data sets are frequently segmented to allow the modeling of individual objects contained in a scanned scene. More complex models, such as computer-aided design models of mechanical parts or models of entire buildings or bridges, are composed of many geometrical primitives, among which a plane is one of the most frequently used; therefore, fitting a plane to range data has been extensively studied [2]–[10]. Modeling is often performed

by fitting a model to point cloud data using a nonlinear least squares (NLS) method [11]–[15]. An important issue is how to propagate an instrument's uncertainty (for example, uncertainty of measured ranges) to the uncertainties of fitted parameters. These uncertainties are essential in quality control processes in which an as-built model (derived from a point cloud) is checked against an as-designed model [16]. The tolerances used in the design process and the uncertainties of the fitted model parameters are both needed to accept the as-built model. For example, the uncertainties of the fitted plane coefficients are needed to check, with a given confidence, if two walls (modeled as a pair of planes) are perpendicular or parallel.

The variance (i.e., squared uncertainty, which, in this paper, we quantify using the standard deviation) of the fitted parameter may be determined in several ways. In one approach, many point clouds are acquired by scanning the same object many times under the same experimental conditions. The same model is then fitted to each data set, yielding many slightly different values of the model parameter. From the ensemble of fitted values, the mean and corresponding variance can be evaluated. This approach does not require explicit knowledge of how the instrument uncertainty propagates into the variances of fitted parameters; however, this approach is very time and labor consuming and, therefore, impractical and rarely used in the field. The other approach is conceptually similar to the previous one, i.e., a model is fitted to many data sets; however, only one data set is actually acquired during the experiment, and the remaining data sets are generated in the computer by perturbing the experimental measurements. This approach is implemented in some commercial software packages, but it is also time consuming and only works well for small data sets. In yet another approach, the variances of the fitted parameters can be evaluated for a single data set, but analytical formulas are needed to propagate the instrument uncertainty into the fitted parameters. In this paper, we compare the outcome of the first and the last approach for fitting a plane to a point cloud. If both approaches give similar values for variances, then we conclude that the analytical formulas are correct; otherwise, they are not.

Closed formulas for the variances of the fitted plane parameters have been derived under the assumption that the uncertainty in the measured range  $r$  is typically much larger than the uncertainty in the angular measurements [17]; thus, the elevation and the azimuth angles,  $\vartheta$  and  $\varphi$ , respectively, are treated as noise-free control variables. This assumption is commonly recognized by users and manufacturers of the instruments from

Manuscript received February 22, 2011; revised April 27, 2011; accepted April 28, 2011. Date of publication July 5, 2011; date of current version December 8, 2011. The Associate Editor coordinating the review process for this paper was Dr. Matteo Pastorino.

The authors are with the National Institute of Standards and Technology, Gaithersburg, MD 20899 USA (e-mail: marek@nist.gov; cheok@nist.gov; kamel.saidi@nist.gov).

Digital Object Identifier 10.1109/TIM.2011.2157720

the class discussed in this paper. We apply the formulas to data sets acquired in a laboratory under many different experimental settings (different target-to-scanner distances, angles of incidence (AOIs), and target reflectivities). In addition, results based on computer simulations were obtained. For every point cloud, a plane was fitted using orthogonal and directional error functions (defined in Section II), yielding two sets of fitted plane coefficients. For most data sets, corresponding plane coefficients obtained with two error functions were different. The fact that different definitions of the error function may lead to different best fit parameters is not surprising. Observed differences may be interpreted as a result of postprocessing bias introduced to the final results by individual error functions. However, this bias is fundamentally different from the bias in collected experimental measurements. The experimental bias (which may be reduced by proper calibration of the measuring instrument) does not affect the variances of the measured parameters. In this paper, we demonstrate for the first time that postprocessing bias, introduced by the choice of error function, can also substantially change the variances of fitted parameters calculated from closed formulas.

This paper is organized as follows. In Section II, a general framework for fitting a plane to point cloud data is revisited, and in Section III, details of data acquisition and computer calculations are discussed. Results are presented in Section IV, followed by a discussion and conclusions in Sections V and VI, respectively.

## II. FITTING A PLANE TO A POINT CLOUD

Points  $\mathbf{P}(x, y, z)$  in a 3-D Cartesian coordinate system lie on a plane when they satisfy the following equation:

$$\mathbf{P}(x, y, z) \bullet \mathbf{w}(\vartheta, \varphi) = D \quad (1)$$

where  $\mathbf{w}(\vartheta, \varphi)$  is a unit vector perpendicular to a plane and  $\bullet$  denotes the dot product of two vectors. Vector  $\mathbf{w}$  may be parameterized by two angles: the elevation  $\vartheta$  and the azimuth  $\varphi$ . The Cartesian coordinates of  $\mathbf{w}(\vartheta, \varphi)$  may thus be written as

$$\mathbf{w}(\vartheta, \varphi) = [\cos \vartheta \cos \varphi, \cos \vartheta \sin \varphi, \sin \vartheta]. \quad (2)$$

The absolute value of parameter  $D$  is the distance from the plane to the origin of the coordinate system that, in this paper, is defined by the location of an instrument. A plane is fitted to the experimental data set  $\mathbf{P}_{\{N\}} = \{\mathbf{P}_j, j = 1, \dots, N\}$ , where  $N$  denotes the number of points. The purpose is to estimate the numerical values of the three parameters defining the plane:  $\vartheta$ ,  $\varphi$ , and  $D$ . Within the framework of the least squares method, the estimated parameters are obtained by minimizing the error function

$$E(\vartheta, \varphi, D, \mathbf{P}_{\{N\}}) = \frac{1}{N} \sum_{j=1}^N E_j^2(\vartheta, \varphi, D, \mathbf{P}_j) \quad (3)$$

where  $E_j$  is the distance between the experimental point  $\mathbf{P}_j$  and its corresponding theoretical point. Different definitions of the theoretical point yield different error functions. In this paper, we study two error functions: the orthogonal error function

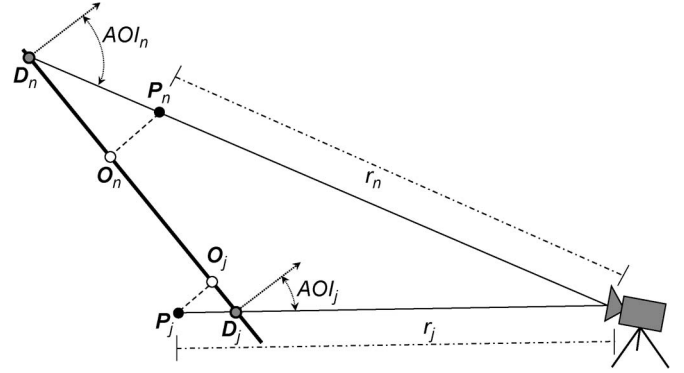


Fig. 1. Measured ranges  $r_n$  and  $r_j$  are affected by uncertainties, and therefore, experimental points  $\mathbf{P}_n$  and  $\mathbf{P}_j$  are not located exactly on (heavy line) a scanned planar surface. Points  $\mathbf{O}_n$  and  $\mathbf{O}_j$  are perpendicular projections of  $\mathbf{P}_n$  and  $\mathbf{P}_j$  onto a plane. Points  $\mathbf{D}_n$  and  $\mathbf{D}_j$  are intersections of rays passing through the instrument and points  $\mathbf{P}_n$  and  $\mathbf{P}_j$  with a plane. Distances  $\mathbf{P}_n\mathbf{O}_n$  and  $\mathbf{P}_j\mathbf{O}_j$  are used in orthogonal fitting while distances  $\mathbf{P}_n\mathbf{D}_n$  and  $\mathbf{P}_j\mathbf{D}_j$  are used in directional fitting. The difference between both fittings depends on the AOI.

$E_O$  and the directional error function  $E_D$ , as explained in Fig. 1 and in the next two sections. Due to the nonlinear dependence of the normal vector  $\mathbf{w}$  on both angles  $\vartheta$  and  $\varphi$ , plane fitting requires nonlinear minimization; however, as is shown in the next two sections, for both error functions  $E_O$  and  $E_D$ , the distance  $E_j$  depends linearly on the third parameter  $D$ . When the error function reaches a minimum, its gradient has to be zero; therefore, distance  $D$  may be explicitly expressed as a function of both angles  $(\vartheta, \varphi)$  and  $\mathbf{P}_{\{N\}}$

$$D \equiv D(\vartheta, \varphi, \mathbf{P}_{\{N\}}). \quad (4)$$

This implies that the original 3-D search space in the minimization problem may be reduced to a 2-D space and the error function may be rewritten as

$$E(\vartheta, \varphi, \mathbf{P}_{\{N\}}) = \frac{1}{N} \sum_{j=1}^N E_j^2(\vartheta, \varphi, \mathbf{P}_j). \quad (5)$$

The location of the minimum for the error function  $E$  depends solely on experimental points  $\mathbf{P}_{\{N\}}$  as follows:

$$\vartheta^* = \vartheta^*(\mathbf{P}_{\{N\}}), \varphi^* = \varphi^*(\mathbf{P}_{\{N\}}), D^* = D(\vartheta^*, \varphi^*, \mathbf{P}_{\{N\}}). \quad (6)$$

As already mentioned in Section I, the range measurement uncertainty is typically much larger than the uncertainty in the angular measurements; thus, an acquired point  $\mathbf{P}_j$  can be expressed as

$$\mathbf{P}_j = r_j \mathbf{p}_j(\vartheta_j, \varphi_j) \quad (7)$$

where  $r_j$  is the range measured at bearings  $(\vartheta_j, \varphi_j)$  and  $\|\mathbf{P}_j\| = r_j$ . In this approximation, the bearings are treated as noise-free control variables, and a unit vector  $\mathbf{p}_j$  is defined as

$$\mathbf{p}_j(\vartheta_j, \varphi_j) = [\cos \vartheta_j \cos \varphi_j, \cos \vartheta_j \sin \varphi_j, \sin \vartheta_j] \quad (8)$$

hence, the analytical formula for the variances of the fitted plane parameters may be derived by applying the uncertainty

propagation formula [18] to (6) as follows:

$$\text{var}(\vartheta^*) \approx \sum_{j=1}^N \left[ \frac{\partial \vartheta^* (\mathbf{P}_{\{N\}})}{\partial r_j} \right]^2 \text{var}(r_j) \quad (9a)$$

$$\text{var}(\varphi^*) \approx \sum_{j=1}^N \left[ \frac{\partial \varphi^* (\mathbf{P}_{\{N\}})}{\partial r_j} \right]^2 \text{var}(r_j). \quad (9b)$$

The analytical formula for the variance of the third parameter  $D^*$  may be obtained from the uncertainty propagation formula applied to the general function  $D(\vartheta, \varphi, \mathbf{P}_{\{N\}})$  defined in (4) as

$$\text{var}(D^*) = \sum_{j=1}^N \left[ \frac{\partial D}{\partial \vartheta} \frac{\partial \vartheta^*}{\partial r_j} + \frac{\partial D}{\partial \varphi} \frac{\partial \varphi^*}{\partial r_j} + \frac{\partial D}{\partial r_j} \right]^2 \text{var}(r_j) \quad (10)$$

where the derivatives of  $D$  are calculated at  $[\vartheta^*, \varphi^*, \mathbf{P}_{\{N\}}]$ . The individual sensitivities  $\partial \vartheta^* / \partial r_j$  and  $\partial \varphi^* / \partial r_j$  used in (9) and (10) and the derivative  $\partial D / \partial r_j$  may be calculated as in [17]. In the aforementioned analytical formulas for  $\text{var}(\vartheta^*)$ ,  $\text{var}(\varphi^*)$  and  $\text{var}(D^*)$ , a variance of the individual measured range  $\text{var}(r_j)$  must be known for each  $j$ . In general, this variance depends on the range  $r_j$ , the AOI, and the reflectivity of the scanned surface; however, the exact dependence is rarely known. Whenever experimental conditions allow neglecting variations of  $\text{var}(r_j)$ , its value may be approximated by the residual value of the error function  $E(\vartheta^*, \varphi^*, \mathbf{P}_{\{N\}})$  if the right model is fitted to the data set (see [19, Ch. 15.1]).

The aforementioned general formulas are applied to two specific error functions: the orthogonal error function  $E_O$  and the directional error function  $E_D$  in the next two sections, respectively.

### A. Orthogonal Error Function

For orthogonal plane fitting (see Fig. 1), the theoretical point  $O_j$  corresponding to the experimental point  $P_j$  is defined as the orthogonal projection of  $P_j$  on a plane. Thus, (3) takes the form

$$E_O(\vartheta, \varphi, D, \mathbf{P}_{\{N\}}) = \frac{1}{N} \sum_{j=1}^N [\mathbf{w}(\vartheta, \varphi) \bullet \mathbf{P}_j - D]^2. \quad (11)$$

Using the condition for zero gradient  $\nabla E_O$ , (4) can be expressed as

$$D(\vartheta, \varphi, \mathbf{P}_{\{N\}}) = \mathbf{w}(\vartheta, \varphi) \bullet \left( \frac{1}{N} \sum_{j=1}^N \mathbf{P}_j \right) = \mathbf{w} \bullet \mathbf{P}_0 \quad (12)$$

where  $\mathbf{P}_0$  is the centroid of all experimental points  $\mathbf{P}_{\{N\}}$ . From the last equation, it follows that the plane fitted with the orthogonal error function has to contain the centroid  $\mathbf{P}_0$ . Substituting (12) into (5) and (11) takes the form

$$E_O(\vartheta, \varphi, \mathbf{P}_{\{N\}}) = \frac{1}{N} \sum_{j=1}^N [\mathbf{w}(\vartheta, \varphi) \bullet (\mathbf{P}_j - \mathbf{P}_0)]^2. \quad (13)$$

### B. Directional Error Function

For the directional plane fitting (see Fig. 1), the theoretical point  $D_j$  corresponding to the experimental point  $P_j$  is defined by the intersection of a ray originating from the instrument (and passing through  $P_j$ ) with the plane as

$$\mathbf{D}_j = t_j \mathbf{P}_j \quad (14)$$

where  $t_j > 0$  is a scalar parameter. If the instrument could measure ranges without error, points  $P_j$  would be located exactly on the plane,  $\mathbf{D}_j = \mathbf{P}_j$ , and  $t_j = 1$ . Range errors are small compared to measured ranges, and therefore,  $t_j$  has values close to one when the fitting parameters are close to their best fit values  $(\vartheta^*, \varphi^*)$ . The theoretical points  $\mathbf{D}_j$  satisfy (1)

$$\mathbf{D}_j(x_j, y_j, z_j) \bullet \mathbf{w}(\vartheta, \varphi) = D. \quad (15)$$

The distance  $E_j$  in (3) is the Euclidian norm, and the directional error function  $E_D$  can thus be written as

$$E_D(\vartheta, \varphi, D, \mathbf{P}_{\{N\}}) = \frac{1}{N} \sum_{j=1}^N \|\mathbf{D}_j - \mathbf{P}_j\|^2 \quad (16)$$

where the parameter  $t_j$  can be calculated from (14) and (15) using the  $\mathbf{p}_j$  defined in (8) as

$$t_j = \frac{D}{r_j \mathbf{w} \bullet \mathbf{p}_j} \quad (17)$$

if the vector  $\mathbf{p}_j$  is not orthogonal to  $\mathbf{w}$ . Two vectors  $\mathbf{p}_j$  and  $\mathbf{w}$  are orthogonal only if the corresponding AOI =  $\pm 90^\circ$ , in which case the theoretical point  $\mathbf{D}_j$  is undefined. For all other AOIs,  $t_j$  can be calculated and substituted into (14). Then, using (8) and the fact that  $r_j = \|\mathbf{P}_j\|$ , (16) yields the following expression for the directional error function:

$$E_D(\vartheta, \varphi, D, \mathbf{P}_{\{N\}}) = \frac{1}{N} \sum_{j=1}^N \left( \frac{D}{\mathbf{w} \bullet \mathbf{p}_j} - r_j \right)^2. \quad (18)$$

Applying the condition for zero gradient  $\nabla E_D$  to (18), (4) can be expressed as

$$D(\vartheta, \varphi, \mathbf{P}_{\{N\}}) = \frac{\sum_{j=1}^N r_j (\mathbf{w} \bullet \mathbf{p}_j)^{-1}}{\sum_{j=1}^N (\mathbf{w} \bullet \mathbf{p}_j)^{-2}}. \quad (19)$$

Equation (5) in this notation can be written as

$$E_D(\vartheta, \varphi, \mathbf{P}_{\{N\}}) = \frac{1}{N} \sum_{j=1}^N \left( \frac{D(\vartheta, \varphi, \mathbf{P}_{\{N\}})}{\mathbf{w}(\vartheta, \varphi) \bullet \mathbf{p}_j} - r_j \right)^2. \quad (20)$$

## III. EXPERIMENT AND DATA PROCESSING

Details of the experimental setup were described in [20]. Here, we briefly summarize the data collection procedure. A square planar target (0.61 m  $\times$  0.61 m) was placed on a holder. Four experimental factors were varied: 1) scanner-to-target distance; 2) reflectivity of target surface; 3) AOI; and 4) relative

TABLE I  
EXPERIMENTAL SETTINGS IN WHICH POINT CLOUDS WERE ACQUIRED IN THE LABORATORY. FOR EACH COMBINATION OF SETTINGS, SCANNING WAS REPEATED THREE TIMES

Scanner to target distance [m]	15	60	110	160
Reflectivity [%]	20	50	75	99
Angle of incidence AOI [°]	0	20	40	60
Relative instrument-target azimuth [°]	< 180		> 180	

azimuth angle between the instrument's nominal direction and a ray passing through the instrument and target center. The first three factors were set at four different levels, and the last one was set at two levels as shown in Table I.

Scanning density was chosen so that the number of points on the target was approximately the same for all AOIs and distances to the scanner ( $N \approx 1600$ ). For each set of experimental conditions, three point clouds were acquired by scanning a target three times.

In addition to point clouds collected with an instrument, data sets were generated from computer simulations. Plane parameters  $(\vartheta_0, \varphi_0, D_0)$  and a target center  $\mathbf{P}_c$  were chosen. For every pair of angles  $(\vartheta_j, \varphi_j)$ , the corresponding noise-free range  $q_j$  was calculated as

$$q_j = \frac{D_0}{\mathbf{w}(\vartheta_0, \varphi_0) \bullet \mathbf{p}_j(\vartheta_j, \varphi_j)} \quad (21)$$

where  $\mathbf{w}$  and  $\mathbf{p}_j$  are defined by (2) and (8). The noisy range  $r_j$  was then calculated as

$$r_j = q_j + \sigma \varepsilon_j \quad (22)$$

where  $\varepsilon_j$  is a pseudorandom number from a normal distribution  $N(0, 1)$  and  $\sigma$  is a scale factor ( $\sigma^2$  approximates constant variance of measured ranges  $\text{var}(r_j)$ ). Spherical coordinates were generated from the simulations and then converted to Cartesian coordinates  $(x_j, y_j, z_j)$ .

A plane was fitted twice to each point cloud, using first the orthogonal error function  $E_O$  and then the directional error function  $E_D$ , defined in (13) and (20). A standard quasi-Newton minimization algorithm as implemented by Davidon–Fletcher–Powell (DFP) in [19] was used in both cases. Thus, for every point cloud, two sets of fitted parameters were obtained:  $(\vartheta_O^*, \varphi_O^*, D_O^*)$  and  $(\vartheta_D^*, \varphi_D^*, D_D^*)$ . Then, for every data set, the variances of the fitted parameters were evaluated using the appropriate analytical formulas (9) and (10) which were applied to the orthogonal and the directional error function. In both (9) and (10), a variance of the measured range  $\text{var}(r_j)$  was approximated by the residual value of the directional error function,  $\text{var}(r_j) \approx E_D(\vartheta_D^*, \varphi_D^*)$ . Finally, all fitted parameters and their respective variances were grouped according to experimental conditions. For each of the 128 combinations of experimental settings (see Table I), the standard deviation of every fitted parameter was calculated from repeated scans. These standard deviations were obtained directly from experimental results, without knowledge of analytical formulas for propagating uncertainties from measured ranges to fitted

parameters. In the following sections, we indicate all these standard deviations with the subscript  $E$

$$\text{std}_E(S^*) = \sqrt{\frac{1}{K(M)} \sum_{m=1}^M (S_m^* - \bar{S}^*)^2} \quad \text{for } S^* = \{\vartheta^*, \varphi^*, D^*\} \quad (23)$$

where  $S_m^*$  is a value of the corresponding plane parameter fitted to the  $m$ th data set while  $\bar{S}^*$  is the average of all  $S_m^*$ ,  $m = 1, \dots, M$ , and all  $M$  data sets were acquired for the same experimental settings. In the laboratory experiments,  $M = 3$ , and in computer simulations,  $M = 100$ ; therefore, we use a corrected estimator (sample standard deviation) with  $K(M) = M - 1$  for data sets acquired in a laboratory and an uncorrected estimator (standard deviation of the sample) with  $K(M) = M$  for computer-generated data sets. This standard deviation was calculated independently for planes fitted with orthogonal and directional error functions, yielding a pair of deviations for each plane,  $\text{std}_E(S_O^*)$  and  $\text{std}_E(S_D^*)$ , respectively. In addition, an average analytical variance was calculated as

$$\overline{\text{var}}(S^*) = \frac{1}{M} \sum_{m=1}^M \text{var}(S_m^*) \quad \text{for } S^* = \{\vartheta^*, \varphi^*, D^*\} \quad (24)$$

where  $\text{var}(S_m^*)$  is the variance calculated from the analytical formula for the  $m$ th data set. Then, a corresponding standard deviation of analytical variances was calculated as

$$\text{std}_A(S^*) = \sqrt{\overline{\text{var}}(S^*)} \quad \text{for } S^* = \{\vartheta^*, \varphi^*, D^*\}. \quad (25)$$

The ratio of the two standard deviations

$$\eta(S^*) = \frac{\text{std}_A(S_O^*)}{\text{std}_E(S_O^*)} \quad \text{for } S^* = \{\vartheta^*, \varphi^*, D^*\} \quad (26)$$

can be used to verify the prediction of the analytical formula for the variance of the fitted plane parameter. If  $\eta \approx 1$ , then the formula is accepted as correct, whereas large deviations from the value of one indicate an incorrect analytical formula. Again, depending on the error function used, two ratios were evaluated:  $\eta(S_O^*)$  and  $\eta(S_D^*)$ . These calculations were repeated for all 128 combinations of experimental settings.

Point clouds generated in computer simulations were processed in a similar manner. In addition, since ground truth parameters  $(\vartheta_0, \varphi_0, D_0)$  were known, the deviations of the plane parameters fitted to the noisy  $m$ th data set could be evaluated as  $\vartheta_{O,m}^* - \vartheta_0$ ,  $\varphi_{O,m}^* - \varphi_0$ ,  $D_{O,m}^* - D_0$  for orthogonal fitting and as  $\vartheta_{D,m}^* - \vartheta_0$ ,  $\varphi_{D,m}^* - \varphi_0$ ,  $D_{D,m}^* - D_0$  for directional fitting.

#### IV. RESULTS

In Fig. 2(a)–(f) and Table II, typical results from fitting a plane to simulated data are shown. Plane parameters  $(\vartheta_0, \varphi_0, D_0)$  were  $(0^\circ, 40^\circ, 8 \text{ m})$ , the center of a target  $\mathbf{P}_c$  was chosen such that the corresponding AOI was equal to  $70^\circ$ , and the standard deviation of the range noise was  $\sigma = 7 \text{ mm}$  in (22).  $M = 100$  noisy data sets were generated, and the deviation  $\Delta S$

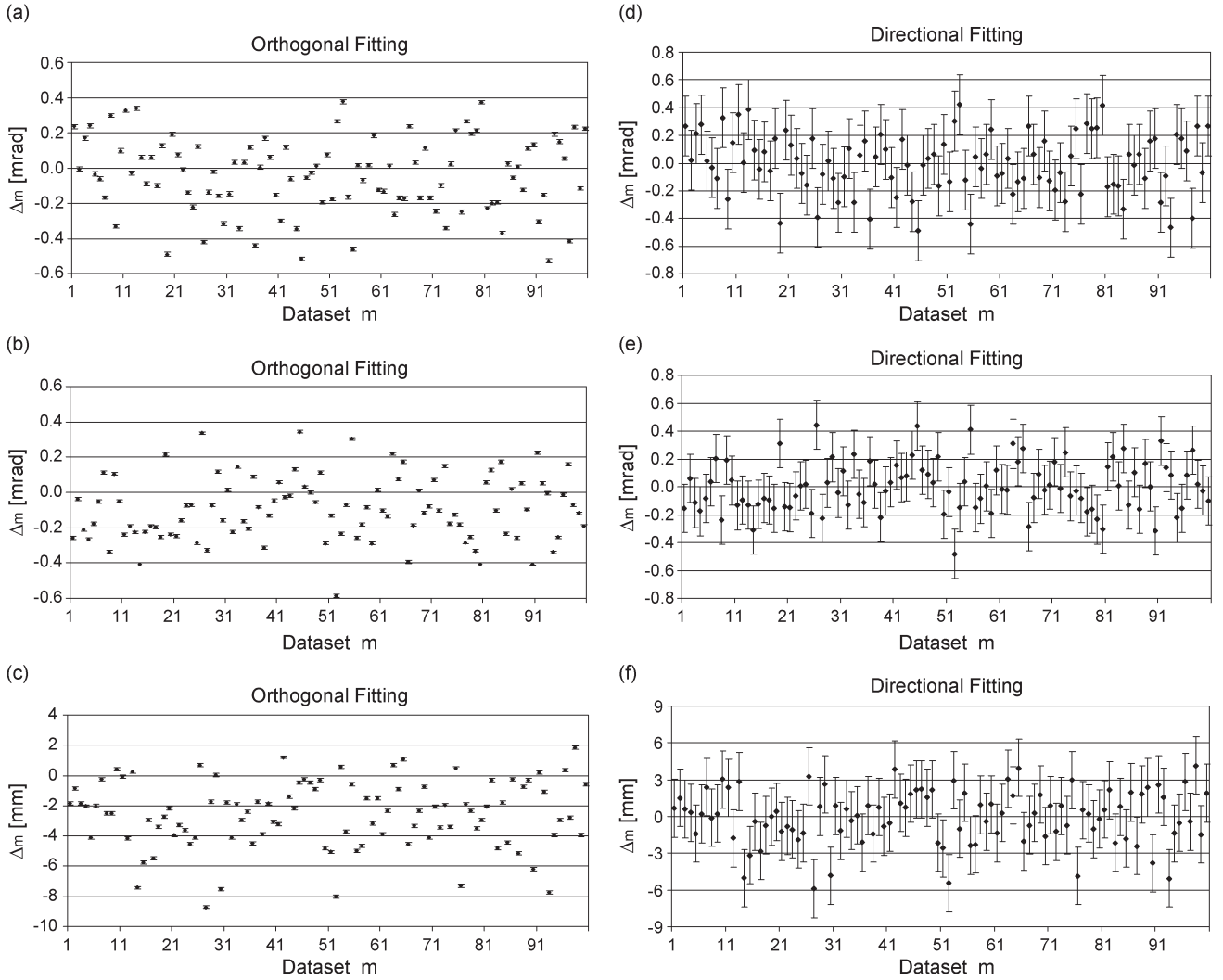


Fig. 2. Deviation  $\Delta_m$  from ground truth of the plane parameters fitted to  $m$ th simulated noisy point cloud using (left column) orthogonal error function and (right column) directional error function. (a)  $\Delta_m = \vartheta_{O,m}^* - \vartheta_0$ . (b)  $\Delta_m = \varphi_{O,m}^* - \varphi_0$ . (c)  $\Delta_m = D_{O,m}^* - D_0$ . (d)  $\vartheta_{D,m}^* - \vartheta_0$ . (e)  $\Delta_m = \varphi_{D,m}^* - \varphi_0$ . (f)  $\Delta_m = D_{D,m}^* - D_0$ . An error bar for each individual point was calculated using the appropriate analytical formulas.

TABLE II  
DEVIATIONS  $\Delta S$  FROM GROUND TRUTH (27), THE EXPERIMENTAL STANDARD DEVIATION  $std_E(S^*)$  (23), AND THE RATIO  $\eta(S^*)$  (26) FOR PLANE PARAMETERS FITTED TO DATA SETS GENERATED IN THE COMPUTER

$\Delta S \pm std_E(S^*)$	$\Delta S = \Delta \vartheta$ [mrad]	$\Delta S = \Delta \varphi$ [mrad]	$\Delta S = \Delta D$ [mm]
$\eta(S^*)$			
Orthogonal	$-0.044 \pm 0.215$	$-0.096 \pm 0.181$	$-2.568 \pm 2.211$
	0.051	0.048	0.049
Directional	$-0.002 \pm 0.213$	$0.00078 \pm 0.180$	$-0.018 \pm 2.186$
	1.011	0.969	1.070

of the average fitted parameter from the corresponding ground truth  $S_0$  was calculated

$$\Delta S = \overline{S^*} - S_0 \quad \text{for } S = \{\vartheta, \varphi, D\}. \quad (27)$$

Results from fitting a plane to experimental point clouds acquired in the laboratory are presented in Fig. 3(a)–(f) and Table III. Error bars for all points shown in Fig. 2(a)–(f) were

calculated using the appropriate analytical formulas. Typically, 10 to 20 iterative steps were needed by the DFP minimization algorithm to converge.

In Fig. 4, a histogram of the ratios of the final values of the orthogonal and the directional error function is shown.

## V. DISCUSSION

Simulated point clouds (generated on a computer) allow the direct comparison of fitted plane parameters to ground truth values ( $\vartheta_0, \varphi_0, D_0$ ). Fig. 2(a)–(c) shows that, for  $M = 100$  noisy data sets (which simulate  $M$  repeated scanning under the same experimental conditions), the orthogonal fitting yields plane parameters which are, on average, statistically different from the ground truth (see Table II). Similar behavior was also observed for another orthogonal error function where individual distances  $E_j$  in (13) were normalized by statistical weights [3]. This behavior has, of course, serious and undesired consequences for the parameters of an as-built model. For example, if the scanner is placed between two walls modeled as a pair of parallel planes, the biases in individual parameters

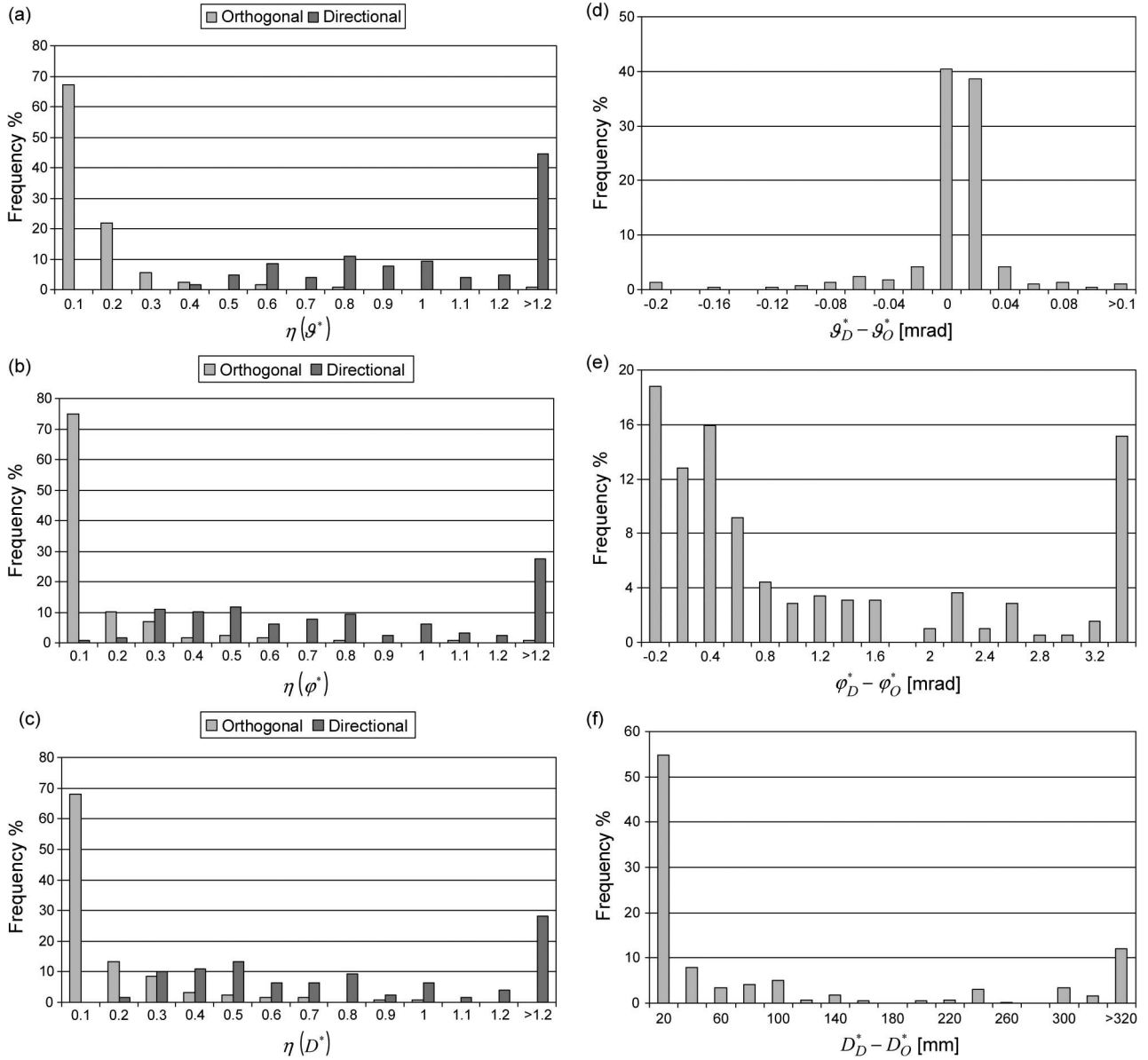


Fig. 3. (Left column) Histograms of ratios  $\eta$  and (right column) differences between fitted parameters obtained from orthogonal and directional fitting calculated from data sets acquired in the laboratory. (a)  $\eta(\vartheta_O^*)$  and  $\eta(\vartheta_D^*)$ . (b)  $\eta(\varphi_O^*)$  and  $\eta(\varphi_D^*)$ . (c)  $\eta(D_O^*)$  and  $\eta(D_D^*)$ . (d)  $\vartheta_D^* - \vartheta_O^*$ . (e)  $\varphi_D^* - \varphi_O^*$ . (f)  $D_D^* - D_O^*$ .

TABLE III  
RESULTS FROM FITTING A PLANE TO POINT CLOUDS ACQUIRED IN THE LABORATORY

Median	$\eta(g^*)$	$\eta(\varphi^*)$	$\eta(D^*)$
Orthogonal	0.071	0.042	0.055
Directional	1.077	0.714	0.713

$D_{O,1}^*$  and  $D_{O,2}^*$  will add up. This will cause the distances between the modeled planes ( $D_{O,1}^* + D_{O,2}^*$ ) to be different from the as-designed model and, depending on the acceptable tolerances, may lead to the rejection of the as-built model. The bias shown in Fig. 2(a)–(c) is not caused by a constant offset in the measured ranges but is introduced to the final results during postprocessing by the choice of an incorrect error function. Table II shows that the same NLS minimization procedure, when applied to the same data set, yields different results for two different error functions.

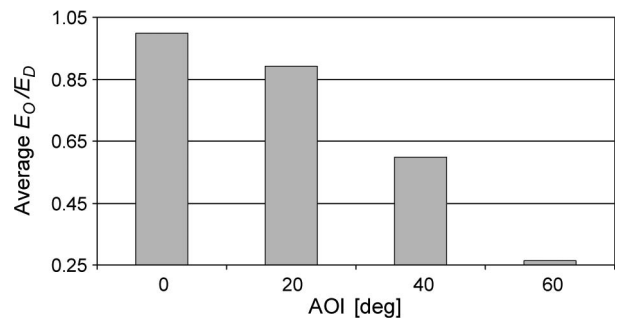


Fig. 4. Histogram of ratios of residual error values  $E_O(\vartheta_O^*, \varphi_O^*)/E_D(\vartheta_D^*, \varphi_D^*)$  averaged over different scanner-to-target distances, reflectivity coefficients, and azimuths between nominal scanner direction and target center, calculated from data sets acquired in the laboratory. Standard deviations for all bars are smaller than 0.02.

The second striking feature visible in Fig. 2(a)–(c) is a clear underestimate of the variances evaluated from the analytical formulas derived from the orthogonal error function. The values

of the ratios  $\eta(\vartheta_D^*)$ ,  $\eta(\varphi_D^*)$ , and  $\eta(D_D^*)$  provided in Table II are much smaller than one.

Contrasting with these observations is the behavior of the directional error function. The deviations  $\Delta S$  of the average fitted plane parameters from their corresponding ground truth are negligibly small, and the values of the ratios  $\eta(\vartheta_D^*)$ ,  $\eta(\varphi_D^*)$ , and  $\eta(D_D^*)$  provided in Table II are close to one. We may conclude that the analytical formulas for variances derived from directional error are correct while the formulas based on the orthogonal error function are not.

The results obtained from fitting a plane to point clouds acquired in the laboratory support the aforementioned conclusions. For almost 80% of the experimental settings, all three ratios  $\eta(\vartheta_D^*)$ ,  $\eta(\varphi_D^*)$ , and  $\eta(D_D^*)$  are smaller than 0.2 [see Fig. 3(a)–(c)]. For directional fitting, almost 60% of all settings yield  $\eta(\vartheta_D^*)$ ,  $\eta(\varphi_D^*)$ , and  $\eta(D_D^*)$  larger than 0.5 and smaller than 1.2. Median values of ratios included in Table III also confirm that directional fitting yields a median closer to one than the orthogonal fitting. Thus, on average, the values calculated from the analytical variances based on the directional error function are much closer to the experimental estimates than the values obtained from the analytical variances based on the orthogonal error function. More detailed inspection of large outliers for  $\eta(\vartheta_D^*)$ ,  $\eta(\varphi_D^*)$ , and  $\eta(D_D^*)$  did not reveal particular experimental conditions for which analytical predictions disagree with experimental estimates. This lack of correlation with any particular experimental conditions may suggest that inaccurate estimate of  $std_E$  from only three repeated scans may be responsible for outliers in  $\eta$ .

In analytical evaluations of variances (9) and (10), we assumed constant variance of measured range  $\text{var}(r_j)$  and approximated it by the residual value of the directional error function  $E_D(\vartheta_D^*, \varphi_D^*)$ . In general, this approximation may not be valid when the size of a scanned planar surface (e.g., a length of scanned wall) is comparable with the distance from the plane center to the instrument. In such situations, the difference between the smallest and the largest AOI in the acquired data set may be large, and the assumption of constant  $\text{var}(r_j)$  may be wrong. Point clouds used in this project were collected in different settings: the width and height of the targets were small relative to the distance to the scanner. Thus, all rays passing through the recorded points  $P_{\{N\}}$  could be approximated as parallel, and the dependence of variance  $\text{var}(r_j)$  on the  $j$ th AOI and range could be neglected.

Fig. 3(d)–(f) show a histogram of the differences between the plane parameters fitted with the orthogonal and the directional error function. For all three plane parameters, the majority of the differences cluster around zero. While the distribution of  $\vartheta_D^* - \vartheta_O^*$  is approximately symmetrical around zero, the distribution of  $\varphi_D^* - \varphi_O^*$  is systematically skewed (i.e., for most of experimental conditions  $\varphi_D^* > \varphi_O^*$ ). The distribution of the third parameter  $D_D^* - D_O^*$  follows the pattern shown in Fig. 3(e) (recall that  $D$  is the distance of the coordinate origin to the fitted plane, not to the target center). Histograms shown in Fig. 3(d)–(f) do not approximate any smooth probability distribution, for example, Gaussian. It is not surprising because the data used to create the histograms were obtained from point clouds acquired in different experimental conditions. Very

large differences between  $D_D^*$  and  $D_O^*$  shown in Fig. 3(f) were observed for large target-to-scanner distances (110 and 160 m), and they clearly illustrate how even small angular differences in the orientation of the normal vector may result in large differences between two fitted planes.

The differences between the orthogonal and the directional fitting are more important for larger AOIs as is shown in Fig. 4.

## VI. CONCLUSION

The results presented in this paper confirm that the choice of error function in fitting a plane to range data is important, particularly for a large AOI. The commonly used orthogonal error function yields fitted plane parameters which are, on average, underestimated. Analytical formulas based on this error function also severely underestimate the values of variances of the fitted plane parameters when compared to experimental estimates based on repeated scans. The directional error function yields fitted plane parameters very close to the ground truth. Analytical formulas based on the directional error function result in variances of fitted parameters that are in agreement with experimental estimates. Thus, the variances may be correctly and quickly determined even for a large single point cloud when the right error function is used in NLS fitting.

The analytical formulas for variances tested in this paper are applicable only to a point cloud acquired from one scanner location. If a data set contains point clouds obtained from different scanner locations and then later registered to a common coordinate system, the formulas cannot be used. Fitting a geometrical model to many data sets acquired from different instrument locations can be performed in two different ways. In the first approach, all point clouds are first registered, and then a model is fitted to one large data set. The advantage of this approach is that more points covering presumably the whole surface of the scanned object are used for fitting. Thus, one may expect that the variances of the fitted parameters would be smaller. The disadvantage of this approach is that the data are contaminated by the registration error. The influence of the registration error on the model parameters fitted to a large data set is not obvious. This is because the common practice of reporting the registration error as the average displacement between corresponding target points is not helpful. In the second approach, a model is fitted first to each point cloud, and then, the average model parameters are calculated. Parameters which are invariant with respect to the coordinate system (for example, the radius of a cylinder or the dimensions of a rectangular box) can be directly averaged; other parameters (like the location of an object or its orientation) need to be first registered to a common coordinate system. It still remains an open question whether the two approaches are equivalent or whether one of them is better and, if so, under what experimental settings.

## REFERENCES

- [1] SPAR, 3D Imaging and Positioning for Design, Construction, Manufacturing, 2009. [Online]. Available: <http://sparllc.com/spar2009.php?page=presentations>
- [2] J. W. Weingarten, G. Gruener, and R. Siegwart, "Probabilistic plane fitting in 3D and an application to robotic mapping," in *Proc. IEEE Int. Conf. Robot. Autom.*, New Orleans, LA, 2004, pp. 927–932.

- [3] Y. Kanazawa and K. Kanatani, "Reliability of fitting a plane to range data," *IEICE Trans. Inf. Syst.*, vol. E78-D, no. 12, pp. 1630–1635, Dec. 1995.
- [4] C. Wang, H. Tanahashi, H. Hirayu, Y. Niwa, and K. Yamamoto, "Comparison of local plane fitting methods for range data," in *Proc. IEEE Comput. Soc. Conf. CVPR*, 2001, pp. I-663–I-669.
- [5] O. Fernandez, "Obtaining a best fitting plane through 3D georeferenced data," *J. Struct. Geol.*, vol. 27, no. 5, pp. 855–858, May 2005.
- [6] S. Wang and Y. H. Tseng, "On the accuracy assessment of least-squares model-image fitting for building extraction from aerial images," presented at the 22nd Asian Conf. Remote Sensing, Singapore, 2001.
- [7] Z. Wang and T. Schenk, "Building extraction and reconstruction from LIDAR data," *Int. Arch. Photogramm. Remote Sens.*, vol. XXXIII, pt. B3, pp. 958–964, 2000.
- [8] S. Wang and Y. H. Tseng, "Model-based building reconstruction from topographic maps and LIDAR data," presented at the Asian Conf. Remote Sensing, Kuala Lumpur, Malaysia, 2007.
- [9] C. M. Huang and Y. H. Tseng, "Plane fitting methods of LIDAR point cloud," presented at the Asian Conf. Remote Sensing, Colombo, Sri Lanka, 2008.
- [10] Y. W. Liu, Y. H. Tseng, and Y. Z. Luo, "Surface feature analysis of ground based LIDAR data," in *Asian Conf. Remote Sensing*, Beijing, China, 2009.
- [11] A. C. Davidson, *Statistical Models*. Cambridge, U.K.: Cambridge Univ. Press, 2003.
- [12] N. R. Draper and H. Smith, *Applied Regression Analysis*, 2nd ed. New York: Wiley, 1981.
- [13] D. A. Freedman, *Statistical Models, Theory and Practice*, revised. Cambridge, U.K.: Cambridge Univ. Press, 2009.
- [14] D. M. Himmelblau, *Process Analysis by Statistical Methods*. New York: Wiley, 1970.
- [15] K. Kanatani, *Statistical Optimization for Geometric Computation*. New York: Elsevier, 1996.
- [16] Y. Turkan, F. Bosche, C. T. Haas, and R. Haas, "Towards automated progress tracking of erection of concrete structures," in *Proc. 6th Int. Conf. Innovation Architecture, Engineering and Construction AEC*, State College, PA, 2010.
- [17] M. Franaszek, "Variances of plane parameters fitted to range data," *J. Res. Nat. Inst. Stand. Technol.*, vol. 115, no. 6, pp. 461–470, Nov./Dec. 2010.
- [18] GUM, Evaluation of Measurement Data—Guide to the Expression of Uncertainty in Measurement, 2008, JCGM. [Online]. Available: <http://www.bipm.org/en/publications/guides/gum.html>
- [19] W. H. Press, S. A. Teukolsky, W. T. Vetterling, and B. P. Flannery, *Numerical Recipes in C*, 2nd ed. Cambridge, U.K.: Cambridge Univ. Press, 1995.
- [20] G. S. Cheok, K. Saidi, M. Franaszek, J. J. Filliben, and N. A. Scott, "Characterization of the range performance of a 3D imaging system," *NIST TN 1695*, 2011.

**Marek Franaszek** received the M.Sc. degree in physics from the Jagiellonian University, Krakow, Poland, and the Ph.D. degree in physics from the Institute of Molecular Physics, Polish Academy of Science, Poznan, Poland, where he worked on deterministic chaos and noise, in 1986.

He is currently with the National Institute of Standards and Technology (NIST), Gaithersburg, MD. Prior to joining NIST in 2007, he was with the National Institutes of Health, Bethesda, MD, where he worked on medical image processing. His current research interests include mathematical modeling and algorithm development for processing data acquired with 3-D imaging systems.

**Geraldine S. Cheok** received the B.S. (*cum laude*) and M.S. degrees in civil engineering from the University of Maryland, College Park, in 1983 and 1986, respectively.

Since 1984, she has been with the National Institute of Standards and Technology, Gaithersburg, MD. Her current research interests include the use of 3-D imaging systems for construction and the development of standards for these systems.

**Kamel S. Saidi** received the Ph.D. degree in civil engineering from the University of Texas, Austin, in 2002, where he focused on information technology at construction sites and construction automation systems.

He is currently with the National Institute of Standards and Technology (NIST), Gaithersburg, MD. His current research includes the development of the Intelligent and Automated Construction Job Site Testbed at NIST as well as the development of performance evaluation methods, metrics, and facilities for 3-D imaging systems.